Lattice study of the two-dimensional Wess-Zumino model

Simon Catterall* and Sergey Karamov
Physics Department, Syracuse University, Syracuse, New York 13244, USA
(Received 2 May 2003; published 8 July 2003)

We present results from a numerical simulation of the two-dimensional Euclidean Wess-Zumino model. In the continuum the theory possesses $N=1$ supersymmetry. The lattice model we employ was analyzed by Golterman and Petcher, who gave a perturbative proof that the continuum supersymmetric Ward identities are recovered without fine-tuning in the limit of vanishing lattice spacing. Our simulations demonstrate the existence of important non-perturbative effects in finite volumes which modify these conclusions. It appears that in certain regions of parameter space the vacuum state can contain solitons corresponding to field configurations which interpolate between different classical vacua. In the background of these solitons supersymmetry is partially broken and a light fermion mode is observed. At fixed coupling the critical mass separating phases of broken and unbroken supersymmetry appears to be volume dependent. We discuss the implications of our results for continuum supersymmetry breaking.

DOI: 10.1103/PhysRevD.68.014503 PACS number(s): 11.15.Ha

I. INTRODUCTION

Supersymmetry has often been invoked as a necessary ingredient for any particle physics theory that attempts to bridge the gap between the scale of electroweak symmetry breaking and the much larger scale associated with unification of the low energy gauge interactions. The basic idea is that while generic field theories involving scalars are unstable to large radiative corrections which mix scales, these radiative effects can be made much smaller if the scalar theory is embedded inside some supersymmetric theory. The dynamical breaking of supersymmetry through non-perturbative effects can then occur at scales which are exponentially suppressed relative to the grand unified scale. This symmetry breaking can, in turn, then trigger electroweak breaking.

Thus the non-perturbative structure of supersymmetric theories is a subject of great interest. The only tool for a systematic investigation of non-perturbative effects is the lattice and so a lot of effort has gone into formulating lattice supersymmetric theories [1,2]. Typically it is difficult to write down lattice actions which can be shown to flow to a supersymmetric fixed point without fine-tuning, as the lattice spacing is reduced.

The model we examine in this paper—the two dimensional Wess-Zumino model—appears to provide an exception to this rule. This theory involves the interactions of scalars and fermion fields and exhibits an $N=1$ supersymmetry in the continuum. A version of this model defined on complex fields and possessing $N=2$ supersymmetry was the subject of a recent numerical study in [3] and was also examined in a variety of earlier papers [4]. The $N=2$ model actually possesses an exact lattice supersymmetry which can be seen to result from its proximity to a continuum topological field theory [5].

We have chosen to study a particular Euclidean lattice formulation of the $N=1$ model due to Golterman and Petcher [1]. The model has also been studied using a Hamiltonian formulation in [6] and [7]. Unlike the Hamiltonian formulations, the Euclidean lattice theory does not retain *any* exact supersymmetry. Nevertheless, Golterman and Petcher prove that the discrete analogues of the continuum supersymmetric Ward identities are satisfied exactly in the limit of vanishing lattice spacing without the necessity of additional fine-tuning. The proof is perturbative and our goal in these simulations was to check whether the model allows for supersymmetry breaking via non-perturbative effects. We find that indeed the lattice model shows evidence of supersymmetry breaking for small values of the lattice mass parameter. Furthermore, this breaking is correlated with the onset of field configurations which sample both the classical vacua of the model. In this limit we also observe a light fermion state which we speculate may play the role of a Goldstino associated with spontaneous supersymmetry breaking.

We have developed and tested a Fourier accelerated version of the so-called R algorithm [8] to handle the fermionic integrations. For details of this Fourier acceleration technique in the context of the hybrid Monte Carlo algorithm we refer the reader to [9]. We have employed an exact algorithm to calculate the sign of the Pfaffian resulting from the integration over the fermion fields. These issues are discussed in detail in Sec. II. We present our evidence for symmetry breaking together with numerical results on the spectrum and Ward identities in Sec. III. In Sec. IV we summarize our findings and discuss their implications for supersymmetry breaking in the continuum in finite and infinite volume.

II. LATTICE MODEL

We consider the on-shell two-dimensional Wess-Zumino model represented by the following continuum action in Euclidean space [1]:

$$S_0=\int d^2x\frac{1}{2}[(\partial_\mu\phi)^2+\bar{\psi}(\partial\!\!\!/+P'(\phi))\psi+P^2(\phi)] \quad (1)$$

where ϕ and ψ are a real scalar field and a two component Majorana spinor respectively. The construction of Euclidean

*Corresponding author. Email address: smc@physics.syr.edu

Majorana spinors is described by Nicolai in [10]. The expression $Q(\phi)=\not{\partial}+P'(\phi)$ will be referred to as the fermion matrix. The potential $P(\phi)$ we consider (actually the derivative of the superpotential) takes the following form depending on a mass M and a coupling constant G:

$$P(\phi)=\begin{cases} M\phi, & G=0, \\ G\phi^2-M^2/4G, & G\neq 0. \end{cases}$$

Notice that this potential is slightly different from the one considered in [1] but may be derived from it by a simple shift in the scalar field. It has the advantage that the total action now depends only on M^2 which allows us to restrict our simulations to positive M. Notice also that the interacting theory has two classical vacua at $\phi=\pm M/2G$. The action (1) is invariant under the following supersymmetry transformation:

$$\delta\phi=\bar{\varepsilon}\psi, \quad \delta\psi=[\not{\partial}\phi-P(\phi)]\varepsilon.$$

The simplest supersymmetric Ward identity following from this invariance takes the form

$$\langle\psi_x\bar{\psi}_y\rangle+\langle[\not{\partial}\phi-P(\phi)]_x\phi_y\rangle=0. \tag{2}$$

Integrating out fermion variables in the path integral leads to the following form of the partition function [11] [see the Pfaffian definition (A1) in the Appendix]:

$$Z=\int D\phi D\psi e^{-S_0}=\int D\phi \ \ \mathrm{sgn}[\mathrm{Pf}(CQ)]e^{\mathrm{tr}[\ln(Q^TQ)]/4-S_b}$$

where C is a Euclidean representation of the charge conjugation matrix and S_b stands for the bosonic part of the action:

$$S_b=\int d^2x\frac{1}{2}[(\partial_\mu\phi)^2+P^2(\phi)].$$

In practice we simulate the system without regard to the sign of the Pfaffian using the following action S:

$$S=-\frac{1}{4}\mathrm{tr}[\ln(Q^TQ)]+\int d^2x\frac{1}{2}[(\partial_\mu\phi)^2+P^2(\phi)]. \tag{3}$$

The expectation values of physical observables are then obtained by reweighting with the measured sign of the Pfaffian in the usual manner:

$$\langle O\rangle_{S_0}=\frac{\langle O\ \mathrm{sgn}[\mathrm{Pf}(CQ)]\rangle_S}{\langle\mathrm{sgn}[\mathrm{Pf}(CQ)]\rangle_S}. \tag{4}$$

We now turn to the lattice model. First, we replace the continuum derivative operator by the symmetric difference matrix $D^\mu_{\mathbf{rr}'}$ where the latter is defined as

$$D^\mu_{\mathbf{rr}'}=\frac{1}{2}[\delta_{\mathbf{r}+\mathbf{e}_\mu,\mathbf{r}'}-\delta_{\mathbf{r}-\mathbf{e}_\mu,\mathbf{r}'}]$$

where $\mathbf{r},\mathbf{r}'$ are two-dimensional vectors enumerating the lattice sites and $\mathbf{e}_\mu$ is a unit vector in the μ direction $\mu=1,2$. In terms of this difference operator the fermion matrix on the lattice can be represented as

$$Q\equiv Q^{\alpha\beta}_{\mathbf{rr}'}=\gamma^\mu_{\alpha\beta}D^\mu_{\mathbf{rr}'}+\delta_{\alpha\beta}P'_{\mathbf{rr}'}$$

where α,β are spinor indices. We have employed the following representations of the Dirac matrices:

$$\gamma_1=\begin{pmatrix}1 & 0\\ 0 & -1\end{pmatrix}, \quad \gamma_2=\begin{pmatrix}0 & -1\\ -1 & 0\end{pmatrix}.$$

The matrix C is given explicitly as

$$C=\begin{pmatrix}0 & -1\\ 1 & 0\end{pmatrix}.$$

It is convenient to define an operator $\Box^n_{\mathbf{rr}'}$:

$$\Box^n_{\mathbf{rr}'}=\frac{1}{2}\sum_\mu[\delta_{\mathbf{r}+n\mathbf{e}_\mu,\mathbf{r}'}+\delta_{\mathbf{r}-n\mathbf{e}_\mu,\mathbf{r}'}-2\delta_{\mathbf{r},\mathbf{r}'}].$$

In particular,

$$\Box^2_{\mathbf{rr}'}=(D^\mu D^\mu)_{\mathbf{rr}'}.$$

In terms of the operator $\Box^n_{\mathbf{rr}'}$ the lattice potential and its derivative can be represented as follows:

$$P_{\mathbf{r}}=\begin{cases} m\phi_{\mathbf{r}}-\Box^1_{\mathbf{rr}'}\phi_{\mathbf{r}'}/2, & g=0, \\ g\phi^2_{\mathbf{r}}-m^2/4g-\Box^1_{\mathbf{rr}'}\phi_{\mathbf{r}'}/2, & g\neq 0, \end{cases}$$

$$P'_{\mathbf{rr}'}\equiv\frac{\partial P_{\mathbf{r}}}{\partial\phi_{\mathbf{r}'}}=\begin{cases} m\delta_{\mathbf{rr}'}-\Box^1_{\mathbf{rr}'}/2, & g=0, \\ 2g\phi_{\mathbf{r}}\delta_{\mathbf{rr}'}-\Box^1_{\mathbf{rr}'}/2, & g\neq 0, \end{cases}$$

where the term with $\Box^1_{\mathbf{rr}'}$ is the Wilson mass operator, which serves to eliminate problems due to doubling of the lattice fermion modes and vanishes in the continuum limit. The dimensionless lattice couplings g and m are related to their continuum counterparts through the relations $g=Ga$ and $m=Ma$ with a the lattice spacing.

Finally the lattice representation of the continuum action (3) can be viewed as the sum of the following boson and fermion components:

$$S_b=\frac{1}{2}\{-\phi_{\mathbf{r}}\Box^2_{\mathbf{rr}'}\phi_{\mathbf{r}'}+P_{\mathbf{r}}P_{\mathbf{r}}\},$$

$$S_f=-\frac{1}{4}\mathrm{tr}[\ln(Q^TQ)]\equiv-\frac{1}{4}[\ln(Q^TQ)]^{\alpha\alpha}_{\mathbf{rr}}.$$

III. SIMULATION DETAILS

To simulate the system (3) we use an importance sampling technique based on a classical evolution of the fields in some auxiliary time. To implement this it is necessary to introduce a Hamiltonian

$$H=\frac{1}{2}p_{\mathbf{r}}p_{\mathbf{r}}+S$$

associated with this auxiliary time variable t and corresponding momentum field p conjugate to the field ϕ. On integration over the auxiliary momentum p it is trivial to show that the classical partition function associated with H reproduces the quantum partition function associated with the original action S. The advantage of this Hamiltonian formulation is that it admits a classical dynamics, which can be used to generate global moves of the field ϕ.

We evolve the system governed by H according to a finite time step leapfrog algorithm in the usual manner:

$$\phi_{t+\delta t}=\phi_t+p_t\delta t+F_t(\delta t)^2/2,$$

$$p_{t+\delta t}=p_t+(F_t+F_{t+\delta t})\,\delta t/2,$$

where F is the force associated with the classical evolution. The ergodicity of the simulation is provided by periodically drawing new momenta p from a Gaussian distribution. In order to decrease the autocorrelation time associated with this dynamics we have utilized acceleration techniques similar to those explored in [9]. Specifically, the discrete time update of the fields corresponding to the Hamiltonian evolution is carried out in momentum space with a momentum dependent time step which is tuned so as to evolve low momentum components of the field more rapidly than high momentum components. Specifically we used a time step of the form

$$\delta t(\mathbf{n})=\epsilon\frac{m_{acc}+4}{\sqrt{\sum_{\mu=1}^{2}\sin^2(2\pi n_\mu/L)+\left(m_{acc}+2\sum_{\mu=1}^{2}\sin^2(\pi n_\mu/L)\right)^2}}$$

where the lattice momenta $\mathbf{n}$ are integer vectors with components ranging from $0\rightarrow L-1$ for an $L\times L$ lattice. The parameter m_{acc} is typically set to the input lattice mass which is close to optimal in these simulations.

The total force can be represented as a sum of boson and fermion contributions:

$$F_{\mathbf{r}}=F^b_{\mathbf{r}}+F^f_{\mathbf{r}}.$$

The evaluation of the boson force is straightforward:

$$F^b_{\mathbf{r}}=-\frac{\partial S_b}{\partial b_{\mathbf{r}}}=\Box^2_{\mathbf{r}\mathbf{r}'}\phi_{\mathbf{r}'}-P_{\mathbf{r}'}P'_{\mathbf{r}'\mathbf{r}}.$$

In order to evaluate the fermion force we first evaluate the following expression involving the fermion matrix:

$$\frac{\partial(Q^TQ)^{\alpha\beta}_{\mathbf{r}\mathbf{r}'}}{\partial b_{\mathbf{s}}}=\frac{\partial^2P_{\mathbf{s}'}}{\partial b_{\mathbf{r}}\partial b_{\mathbf{s}}}Q^{\alpha\beta}_{\mathbf{s}'\mathbf{r}'}+Q^{\beta\alpha}_{\mathbf{s}'\mathbf{r}}\frac{\partial^2P_{\mathbf{s}'}}{\partial b_{\mathbf{r}'}\partial b_{\mathbf{s}}}$$
$$=2g(\delta_{\mathbf{r}\mathbf{s}}Q^{\alpha\beta}_{\mathbf{r}\mathbf{r}'}+Q^{\beta\alpha}_{\mathbf{r}'\mathbf{r}}\delta_{\mathbf{r}'\mathbf{s}}).$$

The fermion force then is

$$F^f_{\mathbf{s}}=-\frac{\partial S_f}{\partial b_{\mathbf{s}}}=\frac{1}{4}[(Q^TQ)^{-1}]^{\alpha\beta}_{\mathbf{r}\mathbf{r}'}\frac{\partial(Q^TQ)^{\beta\alpha}_{\mathbf{r}'\mathbf{r}}}{\partial b_{\mathbf{s}}}$$
$$=g[(Q^TQ)^{-1}]^{\alpha\beta}_{\mathbf{s}\mathbf{r}}Q^{\alpha\beta}_{\mathbf{s}\mathbf{r}}.$$

The computation of the fermion force appears to be problematic as it appears to require the repeated inversion of the fermion matrix, which is prohibitively expensive. In order to resolve this problem we use the so-called R algorithm [8]. The algorithm proceeds by replacing the exact inverse matrix $(Q^TQ)^{-1}$ by a stochastic estimator given by the following expression:

$$[(Q^TQ)^{-1}]^{\alpha\beta}_{\mathbf{r}\mathbf{r}'}\approx\langle X^\alpha_{\mathbf{r}}X^\beta_{\mathbf{r}'}\rangle_N \tag{5}$$

where the vector X is defined through a random Gaussian vector R_g as

$$QX=R_g$$

and the averaging in Eq. (5) is accomplished over N different random noise vectors R_g.

The larger the number N of noise vectors used the more accurate is the evaluation of the inverted matrix in Eq. (5), but the longer computational time the evaluation takes. It is clear that the optimal value of N is given by that which minimizes the error in the inverse matrix for fixed computational time T. Defining the norm of a matrix $\|A\|$ as

$$\|A\|=\sqrt{\sum_{ij}A^2_{ij}}.$$

The relative error is then

$$\frac{\delta\|A\|}{\|A\|}=\sqrt{\frac{N}{T}}\left\{\frac{\delta\|A\|}{\|A\|}\right\}_N$$

where $\{\delta\|A\|/\|A\|\}_N$ is the relative error produced by a single application of an R algorithm with averaging over N noise vectors. Hence the relative error obtained over time T can be characterized by the algorithm efficiency E which we define as

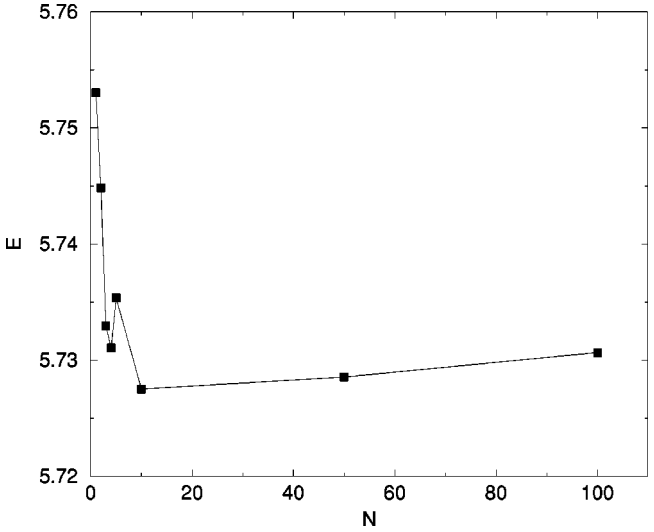

FIG. 1. Algorithm efficiency as a function of the number of noise vectors.

$$E=\sqrt{N}\left\{\frac{\delta\|A\|}{\|A\|}\right\}_N.$$

Our tests showed that this algorithm efficiency does not depend strongly on the choice of N (Fig. 1). Furthermore, we monitored the average bosonic action $\langle S_b\rangle$ and observed no systematic drift with N. Consequently we chose $N=1$ in all our runs. In this limit the corresponding fermion force term yields

$$F^f_{\mathbf{s}}\approx\frac{1}{4}X^\alpha_{\mathbf{r}}X^\beta_{\mathbf{r}'}\frac{\partial(Q^TQ)^{\beta\alpha}_{\mathbf{r}'\mathbf{r}}}{\partial b_{\mathbf{s}}}=\frac{g}{2}Q^{\alpha\beta}_{\mathbf{sr}}(X^\alpha_{\mathbf{s}}X^\beta_{\mathbf{r}}+X^\beta_{\mathbf{s}}X^\alpha_{\mathbf{r}}).$$

Finally let us turn to the issue of the sign of the Pfaffian which results from integrating out the Majorana fields. As we have stressed the simulation action discussed above utilizes the absolute value of this Pfaffian and observables must be re-weighted by the sign of the Pfaffian in order to compute physical expectation values. We have chosen to use an exact algorithm to compute this sign. Since we are in two dimensions and need only do this when making measurements this turns out to be quite manageable in a practical sense. Our procedure was outlined in [12] and for completeness we list the proof and details of the algorithm in the Appendix. In essence the original antisymmetric matrix can be transformed to a special block diagonal form via a similarity transformation built from a triangular matrix. The determinant of the latter can be shown to yield the Pfaffian. We then fold the sign of the Pfaffian in with measurements of observables according to Eq. (4). This reweighting procedure is an effective way to measure expectation values of a variety of observables. However, in certain conditions this technique may fail. The following arguments highlight the problems that may be encountered in this type of situation.

Let N_+ and N_- be the numbers of configurations with positive and negative values of $\mathrm{Pf}(CQ)$ obtained from the simulation of the system (3). Then the average value $\langle O\rangle_{S_0}$ of any physical observable O in the system (1) can be *evaluated* using Eq. (4) as

$$\langle O\rangle=\frac{O_+N_+-O_-N_-}{N_+-N_-} \tag{6}$$

where $O_\pm$ are average values of O obtained in configuration subsets with positive and negative $\mathrm{Pf}(CQ)$. This averaging procedure reveals two statistical problems. The first problem is that if $N_+\approx N_-$ (that is, the probabilities to find the system with either sign of the Pfaffian are approximately the same) then the error of the evaluation (6) experiences an amplification by a large factor $(N_++N_-)/(N_+-N_-)$. In this case it is possible for the error to swamp the signal in the measured value $\langle O\rangle$. Although acquiring more measurements will decrease the fluctuations it might not solve the amplification problem if

$$\lim_{N_++N_-\to\infty}\frac{N_+}{N_-}\sim 1. \tag{7}$$

A second problem is that the expression (6) provides a good evaluation of $\langle O\rangle_{S_0}$ only if $\langle O\rangle$ is uniquely defined in the limit $N_++N_-\to\infty$, which is not necessarily the case. If Eq. (7) takes place then $\langle O\rangle$ is well defined only if $\langle O_+\rangle=\langle O_-\rangle$, which is not guaranteed to be true.

In practice we find that many of our observables suffer large and difficult to quantify errors for small values of the lattice mass where we observe oscillations in the sign of the Pfaffian. This precludes making strong quantitative statements in that region.

IV. RESULTS

We obtained data for lattice sizes $L=8$ and $L=16$ for a fixed lattice coupling $g=0.125$ while varying the lattice bare mass m. The classical vacua of the lattice theory correspond to vanishing fermion field and boson field $\phi=\pm m/2g$. For large m, field configurations which interpolate between these two vacua are associated with large values of the action and are hence expected to be highly suppressed. We thus expect the boson field to be confined in the neighborhood of one of the classical vacua for sufficiently large mass. In the continuum the action is invariant under $\phi\to-\phi$ implying that these two vacuum states are equivalent. This is no longer true on the lattice due to the presence of the Wilson term (actually the sign of the Pfaffian may also change under this symmetry). Indeed our simulations reveal that only the state with $\langle\phi\rangle\sim-m/2g$ survives at large m. As m decreases we expect that tunneling to the other vacuum state may occur and this is indeed seen in our simulations. Figures 2 and 3 show plots of $\langle\mathrm{Pf}(CQ)\rangle$ and $\langle\phi\rangle/m$ versus m for $L=8,16$. Below some critical $m=m_c(L)$ the sign of the Pfaffian, which is negative at large mass m, starts to fluctuate. Additionally, in this region we can see that the average field $\langle\phi\rangle/m$ also undergoes large fluctuations which are the direct result of the Pfaffian sign changes. Indeed, at small mass we observe that for each configuration in our ensemble the sign

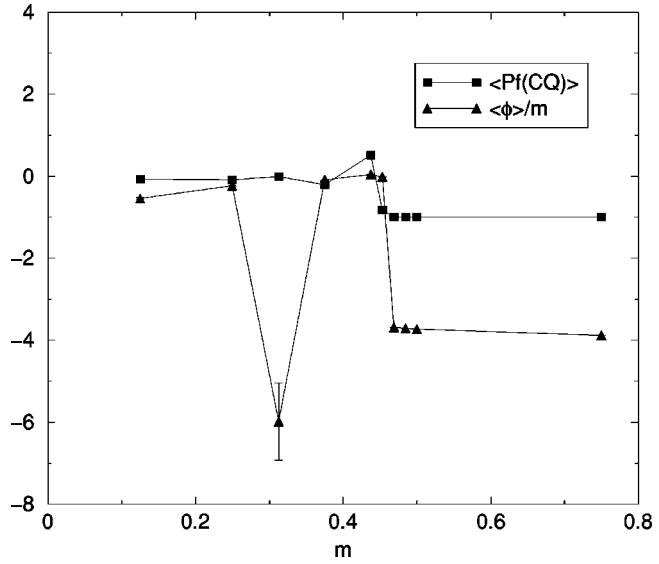

FIG. 2. Average field and average Pf(CQ) for $L=8$. The field values are rescaled for $m<0.46$ by a factor of 1/200.

of the Pfaffian is very accurately correlated with the sign of the mean boson field. Figure 4 shows a time series of both quantities at $m=0.125$ and $L=8$ which illustrates this behavior very well. Actually it is easy to see why this is so. Imagine expanding the Pfaffian as a power series in the boson field ϕ. For sufficiently small m we expect that only the leading term is important and by translational symmetry this can depend only on the field summed over all lattice sites:

$$\mathrm{Pf}(CQ)\sim\sum_{\mathbf{r}}\ \phi_{\mathbf{r}}+O\left(\sum_{\mathbf{rr}}{}'\ \phi_{\mathbf{r}}\phi_{\mathbf{r}'}\right).$$

As we discussed in the previous section this sign oscillation renders accurate measurements of $\langle\phi\rangle$ and its error very difficult in this region.

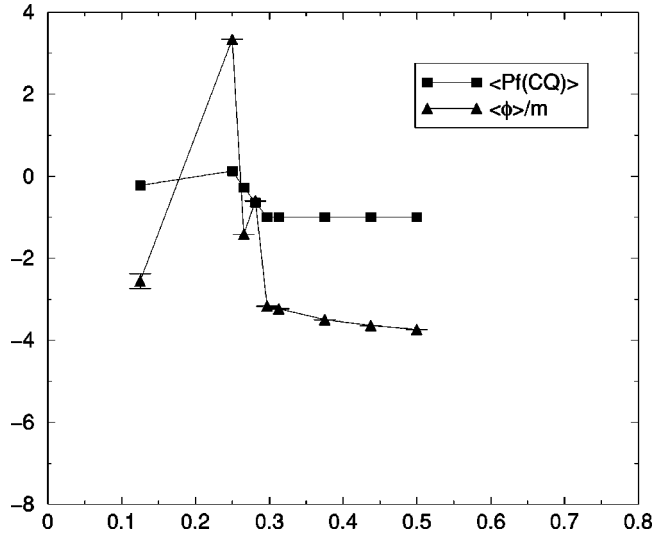

FIG. 3. Average field and average Pf(CQ) for $L=16$. The field values are rescaled for $m<0.29$ by a factor of 1/8.

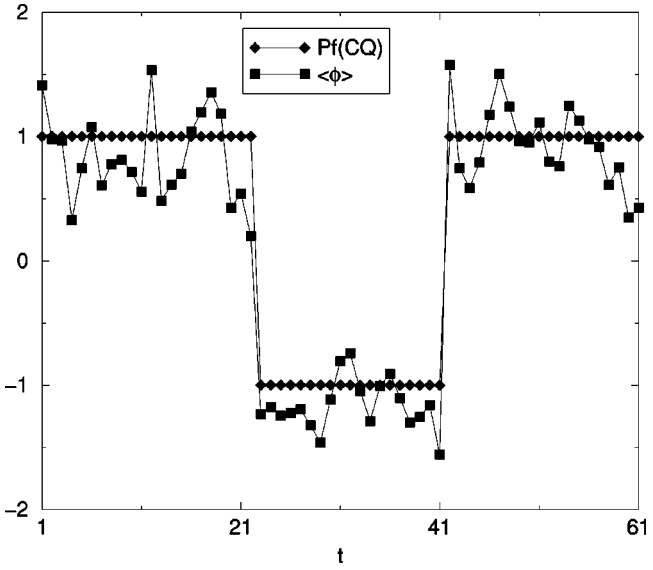

FIG. 4. Evolution of Pf(CQ) and $\langle\phi\rangle$ in auxiliary time t for $L=8$, $m=0.125$.

We have also measured the (zero momentum) boson and fermion correlation functions over the same range of lattice bare masses. Figures 5 and 6 show typical bosonic and fermionic two point functions computed on ensembles corresponding to $L=16$ with $m=0.5$. These are fitted by hyperbolic cosh and mixed hyperbolic sinh and cosh functions to extract the corresponding boson and fermion masses. These (lattice) masses are shown in Figs. 7 and 8 for $L=8$ and $L=16$ respectively. The statistical errors we show neglect the effects of correlation between observables at different time slices. Consider the data for $L=8$. Notice that the boson and fermion masses are equal within statistical errors at large bare input mass but deviate substantially at small mass—the diagonal spinor components of the fermion correlator being dominated by a light state. Contrast this with the off-diagonal components of the fermion correlator for small bare mass which yield a much heavier mass degenerate with the boson

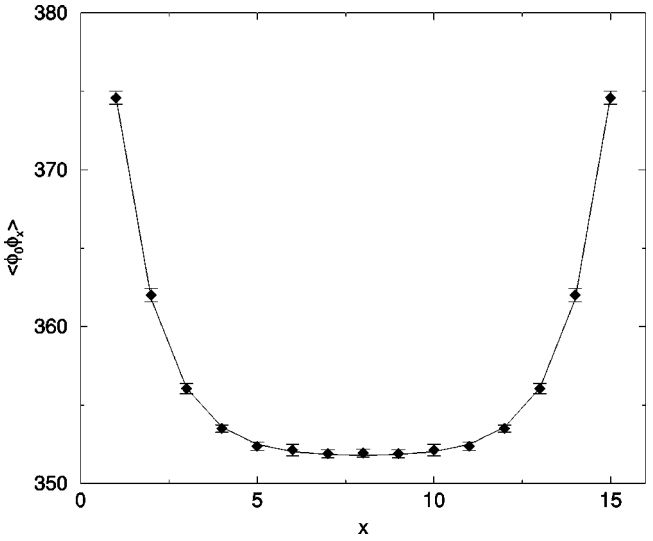

FIG. 5. Bosonic correlation function for $L=16$, $m=0.5$.

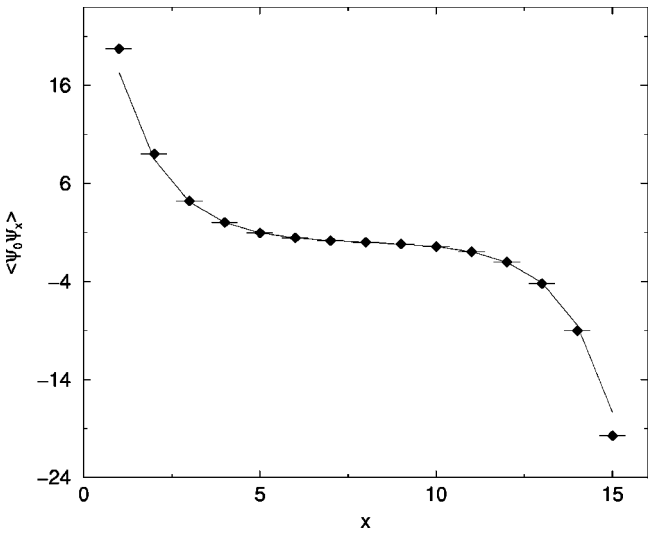

FIG. 6. Fermionic correlation function for $L=16$, $m=0.5$.

mass within statistical errors. A light fermion state is also visible in the $L=16$ data at small mass. The mass of this light fermionic state appears to decrease with increasing bare input lattice mass m. It is tempting to conclude from these observations that for small enough mass supersymmetry breaks as a result of mixing between the two classical vacua—this being signaled by the appearance of a Goldstino.

Another line of evidence in favor of this derives from the partition function itself. On a finite lattice equipped with periodic boundary conditions, such as employed in our simulations, the partition function can be thought of as yielding a representation of the Witten index. Vanishing Witten index is a necessary condition for supersymmetry breaking. But Z can also be related to the expectation value of the sign of the Pfaffian in our simulation ensemble

$$Z_{S_0}=\langle \mathrm{sgn}[\mathrm{Pf}(CQ)]\rangle_S .$$

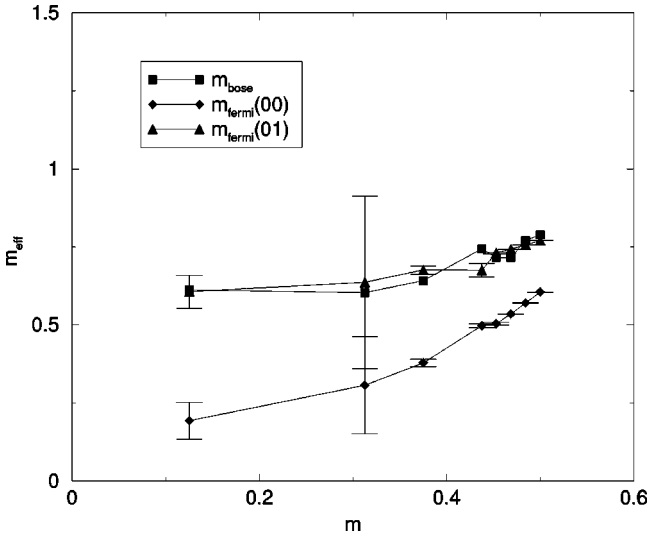

FIG. 7. Mass gaps for $L=8$. Mass gaps from bosonic correlators are shown for $m<0.46$ without error bars.

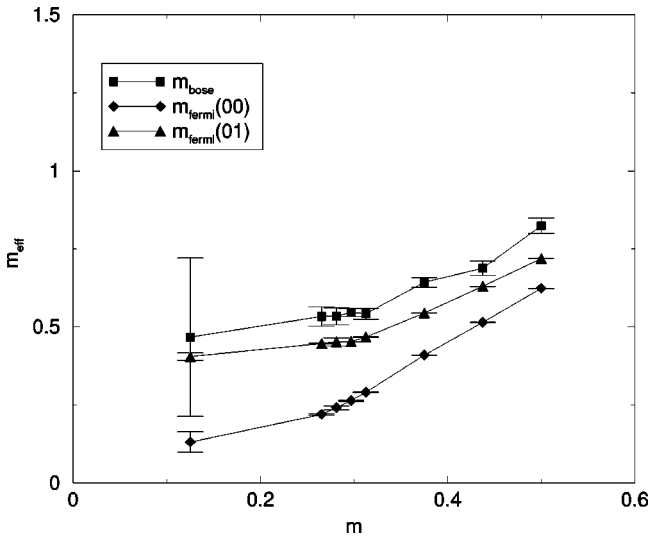

FIG. 8. Mass gaps for $L=16$.

Thus we see that a vanishing partition function would require equal numbers of positive and negative sign Pfaffians in our ensemble. Table I shows the numbers of positive N_+ and negative N_- Pfaffians for three different runs at the same parameter values $L=8$ and $m=0.25$ each containing 100 000 measurements. While the relative errors of on the order of ten percent it should be clear that the data are consistent with a vanishing Witten index.

To investigate this symmetry breaking further we have looked at the simplest supersymmetric Ward identity involving two point functions (2). Figures 9–12 show the bosonic and fermionic diagonal and off-diagonal spinor contributions to this Ward identity together with their sum for two different values of the bare mass $m=0.125$ and $m=0.5$ on a lattice with $L=16$. Clearly for large mass this relation is satisfied within errors for all spinor channels but it is clearly violated at small mass for the channel involving the diagonal spinor correlations. The latter channel is precisely the one in which the light fermion was seen and support the idea that breaking of supersymmetry is associated with the appearance of a Goldstino. Notice that the off-diagonal components of the Ward identity are *still* accurately satisfied even at small mass. We will argue in the next section that this is exactly what we might expect for a partial breaking of supersymmetry associated with the appearance of a finite volume vacuum state composed of solitons.

V. CONCLUSIONS

We have studied a lattice regularized version of the two-dimensional Wess-Zumino model which possesses $N=1$ su-

TABLE I. Numbers of positive and negative Pfaffians for $L=8$ and $m=0.25$.

N_+	N_-
40968	59032
43814	56186
52252	47748

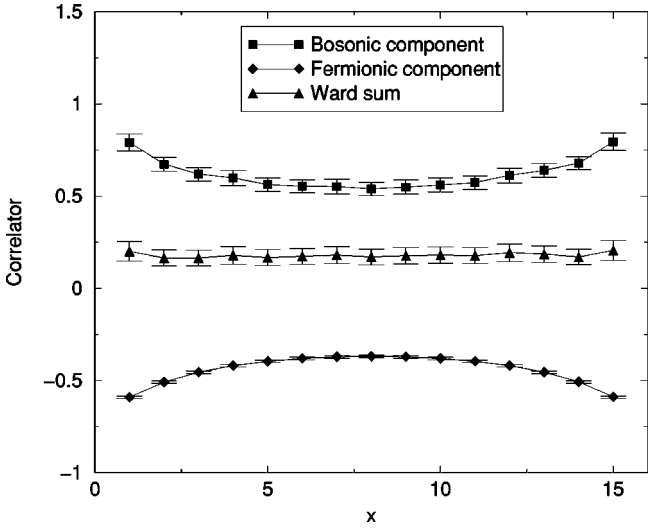

FIG. 9. Contributions to the diagonal components of Ward identity for $m=0.125$.

persymmetry in the naive continuum limit. This model was first analyzed in [1] where it was shown perturbatively that the supersymmetric Ward identities are recovered without fine-tuning in the limit of vanishing lattice spacing. The goal of our simulations was to check these conclusions at the non-perturbative level and to specifically to address the important issue of supersymmetry breaking. We have considered the model for fixed lattice coupling $g=0.125$ and varying lattice mass m for two lattice sizes $L=8$ and $L=16$. For large m our results favor a supersymmetric phase in which boson states pair with equal mass fermion states and the supersymmetric Ward identities are satisfied. In this region of parameter space corresponding to $\phi\sim -m/2g$ the boson field suffers small fluctuations around a single vacuum state.

As the mass is lowered however this picture changes and below some critical mass $m_c(L)$ we see configurations in which the mean boson field varies in sign corresponding to

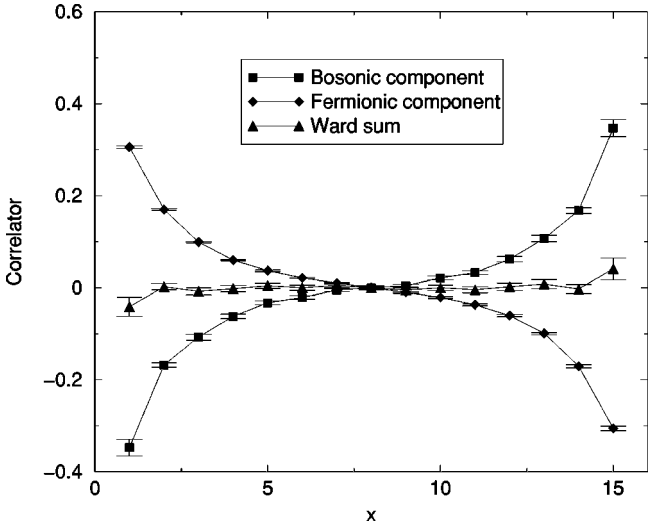

FIG. 10. Contributions to the off-diagonal components of Ward identity for $m=0.125$.

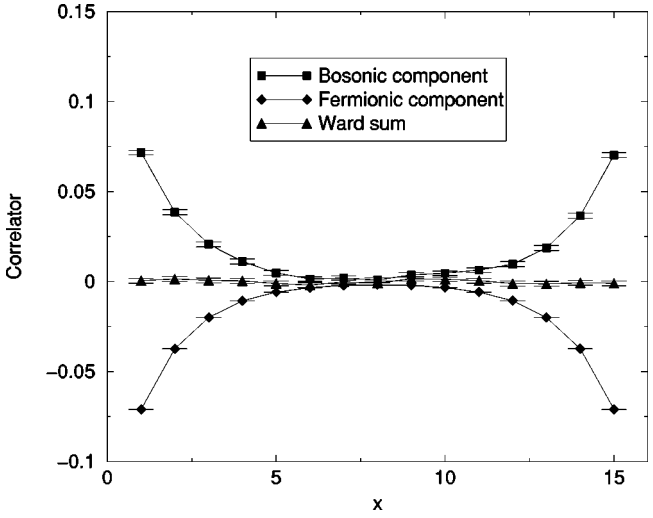

FIG. 11. Contributions to the diagonal components of Ward identity for $m=0.5$.

tunneling between different vacua in auxiliary time. The appearance of states which interpolate between different perturbative vacua is of course entirely a non-perturbative effect. Associated with these tunneling states we see oscillations in the Pfaffian of the fermion operator and the appearance of a light fermion visible in the diagonal components of the fermion correlator. In such a phase it appears that supersymmetry is at least partially broken.

It is possible to get some further understanding of this phenomenon within the context of the semi-classical approximation. Consider first the continuum model. It is clear that *in a finite volume* corresponding to a box of size $L_{\rm phys}$, in addition to the supersymmetric vacua $\phi=\pm M/2G$, there are additional local minima of the action (1) corresponding to domain wall solutions which interpolate between these vacua:

$$\phi(x)\to\begin{cases}\Lambda, & x\to\infty,\\ -\Lambda, & x\to-\infty,\end{cases}$$

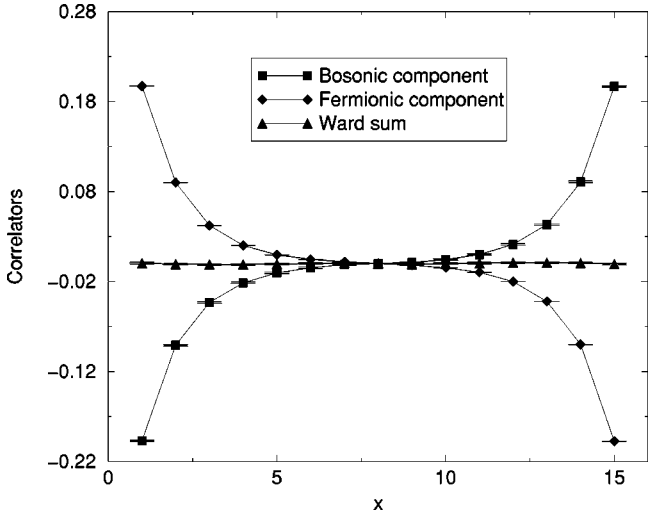

FIG. 12. Contributions to the off-diagonal components of Ward identity for $m=0.5$.

where $\Lambda = M/2G$ and x corresponds to one of the coordinate directions. Indeed, in the continuum, these solutions take the form

$$\phi(x) = \Lambda \tanh[M(x-x_0)/2].$$

While the mass of such a soliton state is non-zero it is possible to show that it is nevertheless annihilated by a single component of the Majorana supercharge and hence such a state preserves one half of the original supersymmetry [13]. This is the origin of our observation that certain components of the Ward identities appear to be satisfied at all values of the parameters. The action of such a soliton is easily evaluated $S_{\rm DW} = \frac{4}{3} G L_{\rm phys} \Lambda^3$ and being proportional to the integral of a total derivative term is topological in character. The corresponding free energy associated with such domain wall solutions then varies as

$$F_{\rm DW} \sim -\ln\left(\frac{L_{\rm phys}}{a}\right) + S_{\rm DW}$$

where the logarithmic variation with linear size arises from the number of ways the domain wall can be introduced into the finite volume. Notice that to do this counting we have to introduce a short distance cut-off a which will naturally be interpreted as a lattice spacing in the discretized model. These arguments lead one to conclude that these non-supersymmetric vacua will dominate over the supersymmetric vacua if

$$\frac{S_{\rm DW}}{L_{\rm phys}} = \frac{M^3}{6G^2} < \left(\frac{\ln(L_{\rm phys}/a)}{L_{\rm phys}}\right). \tag{8}$$

At fixed G this result is in qualitative agreement with our lattice results since it predicts a critical mass $M_C(L_{\rm phys})$ below which supersymmetry would be broken. Translating this result naively into lattice variables leads to the prediction that $m_C \sim 0.3$ for $L=8$ and $g=0.125$, which is quite close to the continuum estimate $M_C a = 0.46$ for $L_{\rm phys} = 8a$. According to our observations this critical mass shifts to smaller values as the lattice size increases which is also in agreement with these analytic arguments. Furthermore, in the vicinity of such a domain wall the fermion is approximately massless and so can play the role of a Goldstino associated with supersymmetry breaking. Notice that these arguments *rely* on the constraint of *finite* volume. The action of such a soliton is unbounded in infinite volume and hence we would naively expect solitons to be completely suppressed in such a limit.

Of course we would like to know whether this finite volume supersymmetry breaking scenario persists in the continuum limit. In general, in *finite* physical volume $V = L_{\rm phy}^2$, the continuum limit $a = L_{\rm phys}/L \to 0$ should be approached by fixing (in this case) two renormalized physical parameters which may be taken as the mass $M_R L_{\rm phy}$ and coupling constant $G_R L_{\rm phy}$—expressed in units of the physical length $L_{\rm phy}$. Perturbation theory allows us to relate these renormalized dimensionless quantities to their bare lattice counterparts

$$G_R L_{\rm phy} \sim gL, \quad M_R^2 L_{\rm phy}^2 \sim m^2 L^2 - C g^2 L^2 \ln(\mu a)$$

where μ is the mass scale associated with the renormalization point and C is a numerical constant. Along such an renormalization group trajectory the value $\lambda = m/2g$ can then be related to its constant (continuum) value Λ_R via the relation

$$\Lambda_R^2 \sim \lambda^2 \left[1 - \frac{C}{\lambda^2} \ln\left(\frac{\mu L_{\rm phys}}{L}\right)\right].$$

In finite volume the renormalization point in units of the IR cutoff $\mu L_{\rm phys}$ should be held constant. There are then three limiting behaviors possible for the system. For small enough L the logarithm is large and positive corresponding to a negative value of Λ_R^2 and a non-zero vacuum energy. For $L \sim L_c = \mu L_{\rm phys} e^{-\lambda^2}$ the logarithmic term is small, Λ_R is now positive but the free energy of a soliton configuration is negative and hence the vacuum energy will still be non-zero. Thus for any value of the bare parameters and any renormalization point supersymmetry breaking will occur for small enough lattice size. Conversely for large enough L the log term will dominate and lead to an infinite soliton action as $L \to \infty$ for any value of the bare parameters. In this limit the solitons should disappear and supersymmetry should be restored. These conclusions are in agreement with the reasoning presented in [14].

While this work was in preparation we received a report [15] in which the same model is studied in a Hamiltonian framework. The conclusions of this study are broadly in agreement with ours.

ACKNOWLEDGMENTS

Simon Catterall was supported in part by DOE grant DE-FG02-85ER40237.

APPENDIX: THE ALGORITHM FOR DETERMINING THE PFAFFIAN OF AN ANTISYMMETRIC MATRIX

In this appendix we describe the algorithm for determining the Pfaffian of an arbitrary antisymmetric $2N \times 2N$ matrix M, which is defined as follows:

$$\mathrm{Pf}M = \frac{1}{N! 2^N} \varepsilon_{\alpha_1,\beta_1,\ldots,\alpha_N,\beta_N} M_{\alpha_1,\beta_1} \ldots M_{\alpha_N,\beta_N}. \tag{A1}$$

The algorithm utilizes the following theorem.

Theorem. If P is a matrix such that an antisymmetric matrix M can be represented as $M = P^T J P$ where $J = \mathrm{diag}(i\gamma_3, i\gamma_3, \ldots, i\gamma_3)$ is a block-diagonal matrix then $\mathrm{Pf}M = \det P$ (here $C = i\gamma_3$ is the Euclidean representation of the charge conjugation matrix for a two-dimensional system).

The theorem can be proved using the representation of the Pfaffian in terms of an integral over a Grassmann $2N$ vector θ. Defining $\tilde{\theta} = P\theta$ we have

$$\mathrm{Pf}M \equiv \int d\theta e^{-\theta^T M\theta/2} = \int d\theta e^{-\theta^T P^T JP\theta/2} = \int d\theta e^{-\tilde{\theta}^T J\tilde{\theta}/2} = \int d\theta \frac{1}{N!}[\tilde{\theta}_{2n-1}\tilde{\theta}_{2n}]^N = \int d\theta \frac{1}{N!}[P_{2n-1,\alpha}\theta_\alpha P_{2n,\beta}\theta_\beta]^N$$

$$= \int d\theta P_{1,\alpha_1}\theta_{\alpha_1} P_{2,\beta_1}\theta_{\beta_1}\cdots P_{2N-1,\alpha_N}\theta_{\alpha_N} P_{2N,\beta_N}\theta_{\beta_N} = \varepsilon_{\alpha_1,\beta_1,\ldots,\alpha_N,\beta_N} P_{1,\alpha_1} P_{2,\beta_1}\cdots P_{2N-1,\alpha_N} P_{2N,\beta_N} = \det P.$$

Notice that the matrix P is not orthogonal ($P^T \neq P^{-1}$); hence it is not associated with any basis transformation in $2N$-dimensional vector space.

The above theorem can be given an alternative formulation. Defining $Q = P^{-1}$ leads to the following statement: if $Q^T M Q = J$ then $\mathrm{Pf}M = (\det Q)^{-1}$. This formulation is used in the algorithm we describe below. The purpose of the algorithm is to represent a given antisymmetric matrix M in terms of a triangular matrix Q so that the $\det Q$ and hence the $\mathrm{Pf}M$ can be found easily.

The algorithm task. Given an arbitrary antisymmetric $2N\times 2N$ matrix M find a triangular matrix Q such that $Q^T M Q = J$, $J = \mathrm{diag}(i\gamma_3, i\gamma_3, \ldots, i\gamma_3)$.

The triangular matrix $Q = \{q_i\}$ represented in terms of its columns q_i will satisfy the relation above *if and only if* its columns satisfy the following conditions:

$$(q_{2i-1} M q_{2j-1}) = 0, \quad (q_{2i} M q_{2j}) = 0,$$

$$(q_{2i} M q_{2j-1}) = -(q_{2j-1} M q_{2i}) = \delta_{ij}.$$

The following algorithm by construction leads to such a matrix Q.

The algorithm.

(1) Establish a unary $2N\times 2N$ matrix $Q = \mathrm{diag}\{1,1,\ldots,1\} = \{e_i\}$, where unary vectors e_i are columns of Q, $i = 1,2,\ldots,2N$.

(2) For odd values $i = 1,3,\ldots,2N-1$ repeat the following steps:

(a) Leave e_i as is.

(b) Redefine $e_{i+1} \to e_{i+1}/(e_{i+1} M e_i)$.

(c) For $k = i+2, i+3, \ldots, 2N$ redefine $e_k \to e_k - e_i(e_{i+1} M e_k) + e_{i+1}(e_i M e_k)$.

Notice that in 2(c) the vector e_{i+1} is used after it is redefined in 2(b).

[1] Maarten F.L. Golterman and Donald N. Petcher, Nucl. Phys. **B319**, 307 (1989).

[2] P. Dondi and H. Nicolai, Nuovo Cimento Soc. Ital. Fis., A **41**, 1 (1977); S. Elitzur, E. Rabinovici, and A. Schwimmer, Phys. Lett. **119B**, 165 (1982); J. Bartels and J. Bronzan, Phys. Rev. D **28**, 818 (1983); T. Banks and P. Windey, Nucl. Phys. **B198**, 226 (1982); I. Montvay, *ibid.* **B466**, 259 (1996); Golterman and Petcher [1]; W. Bietenholz, Mod. Phys. Lett. A **14**, 51 (1999); A. Feo, hep-lat/0210015.

[3] S. Catterall and S. Karamov, Phys. Rev. D **65**, 094501 (2002).

[4] N. Sakai and M. Sakamoto, Nucl. Phys. **B229**, 173 (1983); S. Elitzur and A. Schwimmer, *ibid.* **B226**, 109 (1983); H. Nicolai, Phys. Lett. **89B**, 341 (1980).

[5] S. Catterall, "Lattice Supersymmetry and Topological Field Theory," hep-lat/0301028.

[6] M. Beccaria, M. Campostrini, and A Feo, Nucl. Phys. B (Proc. Suppl.) **106**, 944 (2002).

[7] M. Beccaria, M. Campostrini, and A. Feo, "A Hamiltonian Lattice Study of the two-dimensional Wess-Zumino Model," in Proceedings of Lattice 2002, hep-lat/0209010.

[8] Steven Gottlieb, W. Liu, D. Toussaint, R.L. Renken, and R.L. Sugar, Phys. Rev. D **35**, 2531 (1987).

[9] S. Catterall and S. Karamov, Phys. Lett. B **528**, 301 (2002).

[10] H. Nicolai, Nucl. Phys. **B156**, 177 (1979).

[11] Istvan Montvay, "Majorana Fermions on the Lattice," Report No. DESY-01-113, 2001, hep-lat/0108011.

[12] I. Campos, A. Feo, R. Kirchner, S. Luckmann, I. Montvay, G. Münster, K. Spanderen, and J. Westphalen, Eur. Phys. J. C **11**, 507 (1999).

[13] E. Witten and D. Olive, Phys. Lett. **78B**, 97 (1978).

[14] E. Witten, Nucl. Phys. **B202**, 253 (1982).

[15] M. Beccaria and C. Rampino, "World-Line Path Integral Study of Supersymmetry Breaking in the Wess-Zumino Model," hep-lat/0303021.